American Mineralogist, Volume 84, pages 288–293, 1999

Normal and inverse ringwoodite at high pressures

Boris Kiefer,[1] Lars Stixrude,[1] and Renata Wentzcovitch[2]

[1]Department of Geological Sciences, University of Michigan, Ann Arbor, Michigan 48109-1063, U.S.A.
[2]Department of Chemical Engineering and Materials Science, Minnesota Supercomputer Institute, University of Minnesota, Minneapolis, Minnesota 55455, U.S.A.

Abstract

We present a first-principles computational study of the structural properties of ringwoodite and the influence of cation exchange on these properties as well as the enthalpy differences between ringwoodite and inverse ringwoodite. Our results agree with low-temperature experiments, in that cubic ringwoodite is the stable structure up to 25 GPa. This pressure range encompasses the lower part of the mantle transition zone where ringwoodite is thought to be the most abundant phase. The equation of state as derived from experiment and theory are in good agreement. In contrast to normal ringwoodite, inverse ringwoodite compresses highly anisotropically and the compression mechanisms differ considerably for the two structures. The predicted enthalpy difference between normal and inverse ringwoodite is significantly smaller than that obtained from a simple ionic model (O'Neill and Navrotsky 1983), emphasizing the importance of including structural relaxation in models that address the energetics of order-disorder reactions, at least in the case of ringwoodite.

Introduction

Ringwoodite is thought to be the most abundant mineral in the lower part of the transition zone (Ringwood 1958; Ita and Stixrude 1992), which implies that its physical properties should determine those of the mantle at this depth (520–660 km) to a first approximation. Experiments show that ringwoodite has cubic symmetry at low temperatures (Meng et al. 1994). However, the cation distribution of Mg and Si over tetrahedral and octahedral sites (normal-inverse) is poorly constrained because the X-ray scattering factors for Mg and Si are similar. Even if the cation distribution in ringwoodite were known at low temperatures, this would not necessarily represent transition zone conditions, due to the high temperatures at this depth (in excess of 1500 °C). For these reasons, the symmetry of ringwoodite at transition zone conditions is still unknown. Knowing the symmetry is important because the cation distribution in ringwoodite is expected to influence substantially its physical properties, particularly on the elastic constants, which are critical for correlating seismic anisotropy and mantle flow (Karato 1997) in this depth range.

Experimental and theoretical efforts were used to describe the state of ringwoodite at pressure and temperature conditions representative of the lower part of the transition zone. Hazen et al. (1993) analyzed X-ray diffraction patterns from quenched samples that were prepared under transition zone conditions. Systematic deviations of the Si-O bondlength from an average value in silicates was associated with 4% Mg occupancy in the tetrahedral site. O'Neill and Navrotsky (1983) assumed that disorder has no effect on the crystal symmetry or cell shape of ringwoodite. Consequently they described Mg/Si disorder in the experimentally determined (cubic) low temperature structure of ringwoodite. Using bond length systematics and experimentally measured cation distributions, they concluded that only a very small amount of cation disorder is present at transition zone temperatures. However, in both cases, the effects of pressure were not considered and the amount of disorder was inferred only indirectly from bond length systematics. The amount of disorder might also change during the quench process, and it is therefore not clear how the results apply to the mineralogy in the lower part of the transition zone.

We performed first-principles calculations to investigate the influence of cation exchange on the physical properties of ringwoodite. This method is very well suited to evaluate these changes because we can specify the atomic arrangement, allowing us to characterize the system uniquely in terms of cation exchange with respect to a reference configuration. The calculations do not require any experimental input and allow us to follow changes in the system on an atomic scale. We consider two end-members to evaluate the influence of cation exchange on physical properties: normal and inverse ringwoodite. We performed full structural optimizations for both structures to evaluate differences in the equation of state, compression mechanisms, and the relative stability of the two structures as a function of pressure up to 25 GPa, which encompasses the lower part of the transition zone.

0003–004X/99/0003–0288$05.00

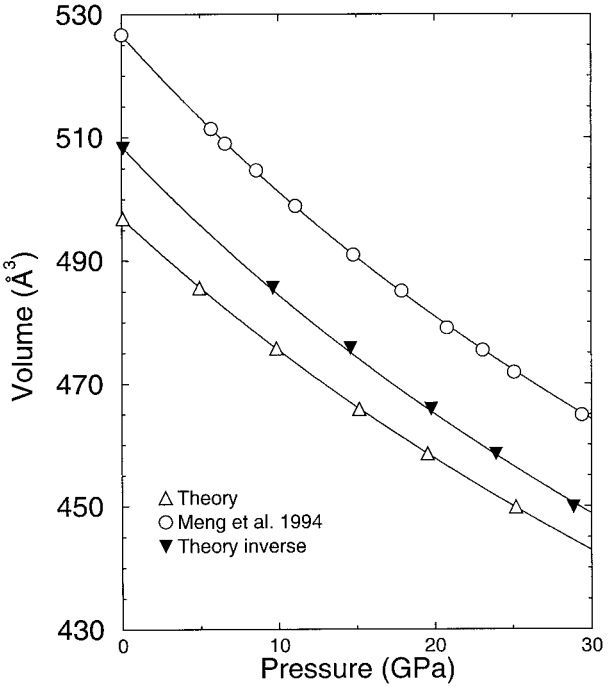

FIGURE 1. Static equation of state as derived from theory for normal and inverse ringwoodite and from experiment extrapolated to 0 K (Meng et al. 1994) for cubic ringwoodite.

METHOD

We have used a first-principle variable-cell-shape-molecular-dynamics strategy (Wentzcovitch et al. 1993) to obtain the ground state structural configurations at arbitrary pressures. This technique combines density functional theory (Kohn and Sham 1965) in the framework of the pseudopotential plane-wave method (Cohen 1982; Pickett 1989), with a classical molecular dynamics strategy (Wentzcovitch 1991), which allows for efficient minimization of forces and stresses through simultaneous relaxation of all structural parameters. With the dynamics operating in damped mode, it requires typically 15 to 25 time steps to reach equilibrium configurations. This technique has been successfully applied to study the pressure dependence of structural and elastic properties of several mantle silicates in the past (Wentzcovitch and Price 1996; Wentzcovitch and Stixrude 1997; Kiefer et al. 1997).

We use the same Troullier-Martins pseudopotentials (Troullier and Martins 1991) for Mg, Si, and O, as in previous calculations on forsterite (Wentzcovitch and Stixrude 1997). The Ceperley-Alder parameterization for the LDA was used (Ceperley and Alder 1980). Convergence tests for ringwoodite and inverse ringwoodite have shown that reliable results can be obtained for a basis set that contains plane waves up to a kinetic energy of E_{cut} = 70 Ry. Our results were obtained with one k-point in the irreducible wedge of the Brillouin zone at (¼, ¼, ¼), corresponding to a 2 × 2 × 2 Monkhorst-Pack grid (Monkhorst and Pack 1976).

TABLE 1. Equation-of-state

	Mg-spinel			Inverse Mg-spinel
System	Experiment (300 K)*	Experiment†	Theory‡	Theory‡
V_0 [Å^3]	526.7	523.9	497.0	509.2
K_0 [GPa]	182.0	190.3	206.8	184.0
K_0'	4.2	4.1	4§	4§

* Meng et al. (1994) at 300 K.
† Meng et al. (1994) extrapolated to 0 K.
‡ At 0 K.
§ Assumed value.

Structure refinements for ringwoodite at low temperature show that it is cubic and has symmetry $Fd\bar{3}m$ with Z = 8 Mg_2SiO_4 units in the conventional unit cell. Inverse ringwoodite, with all Si in the octahedral site and Mg split equally between tetrahedral and octahedral sites, has not been found in laboratory experiments. We have chosen the structure of another spinel, Mg_2TiO_4, that has an inverse content of 90% at low temperatures. The structure is tetragonal, with spacegroup $P4_122$ and Z = 4 formula units in the unit cell (Wechsler and von Dreele 1989). To describe normal ringwoodite in the symmetry of inverse ringwoodite, the tetragonal a-axis is rotated 45° with respect to the conventional cubic axes leading to $a_{inverse} = 1/\sqrt{2}\ a_{normal}$ and $c_{inverse} = a_{normal}$ and an ideal c/a ratio of $\sqrt{2}$, where a_{normal} is the lattice parameter of the conventional unit cell.

To compare precisely the enthalpies of normal and inverse ringwoodite, both structures must be described in the same supercell. This representation is necessary to eliminate the offset in the enthalpies due to differences in the basis-sets used for the calculation of the electronic band structure in $Fd\bar{3}m$ and $P4_122$ symmetry. Because $P4_122$ is a subgroup of $Fd\bar{3}m$, it was sufficient to perform all calculations in the lower $P4_122$ symmetry.

RESULTS

Equation-of-state and structure

For ringwoodite, our calculations yield a zero-pressure, zero-temperature volume that is 5.7% smaller and a bulk modulus that is 13% larger than those determined by experiments at 300 K (Fig. 1 and Table 1). Meng et al. (1994) determined the equation of state for ringwoodite at 300 K and 700 K. The values for V_0, K_0, and K_0' at both temperatures have been used to extrapolate the experimental results linearly to 0 K (Table 1). This extrapolation reduces the difference in volume and bulk modulus between theory and experiment to 5.1 and 8.7%, respectively. The remaining difference can be attributed to the LDA approximation that typically overbinds structures. In the case of Mg-spinel, this leads to Mg-O and Si-O bond lengths that are 2.4 and 0.6% too small, respectively, as compared to experiment (Table 2).

The zero pressure volume of inverse ringwoodite is larger as compared to ringwoodite by 2.5% (Fig. 1, Table 1). To address the question of how the cell shape of in-

TABLE 2. Polyhedral geometry

Polyhedra	Mg-spinel Experiment (300 K)*	Mg-spinel Theory†	Inverse Mg-spinel Theory†
Octahedral coordination			
Mg-O [Å]	2.070	2.021	2.024
Poly. Vol. [Å^3]	11.78	10.99	10.51
Q.E	1.0026	1.0061	1.0336
Ang. Var. [degree^2]	8.95	5.60	123.84
Si-O [Å]	–	–	1.786
Poly. Vol. [Å^3]	–	–	7.43
Q.E	–	–	1.0087
Ang. Var. [degree^2]	–	–	28.68
Tetrahedral coordination			
Mg-O [Å]	–	–	1.927
Poly. Vol. [Å^3]	–	–	3.68
Q.E	–	–	1.0065
Ang. Var. [degree^2]	–	–	25.35
Si-O [Å]	1.655	1.645	–
Poly. Vol. [Å^3]	2.33	2.28	–
Q.E	1.0000	1.0000	–
Ang. Var. [degree^2]	0.00	0.22	–

* Sasaki et al. (1981) at room temperature.
† At 0 K.

verse ringwoodite changes with pressure, we calculated the *c*/*a* ratio from our fully optimized structures (Fig. 2). The deviations from the cubic parent structure increase with increasing pressure (c/a differs by 6.2% from ideal at 20 GPa). This behavior contrasts with the assumption by O'Neill and Navrotsky (1983) that cation exchange and disorder do not affect the crystal symmetry and the cell shape.

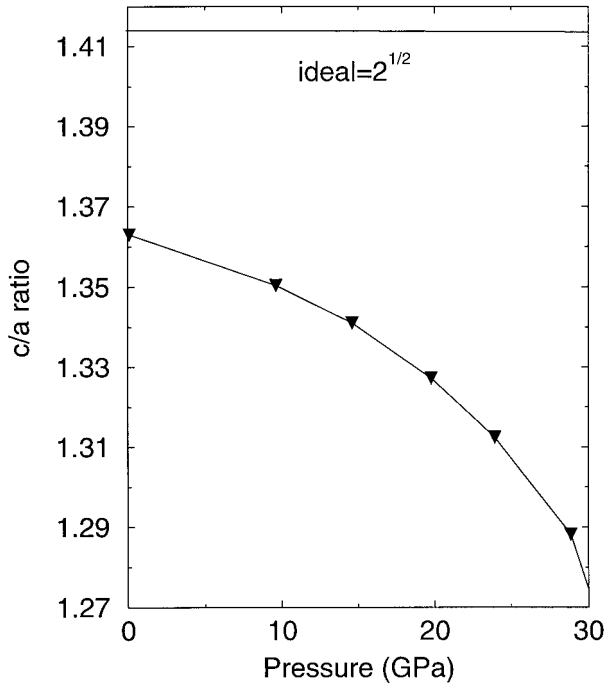

FIGURE 2. *c*/*a*-ratio at 0 K for tetragonal inverse ringwoodite (line with triangles). For the ideal cubic structure $c/a = \sqrt{2}$ (solid line).

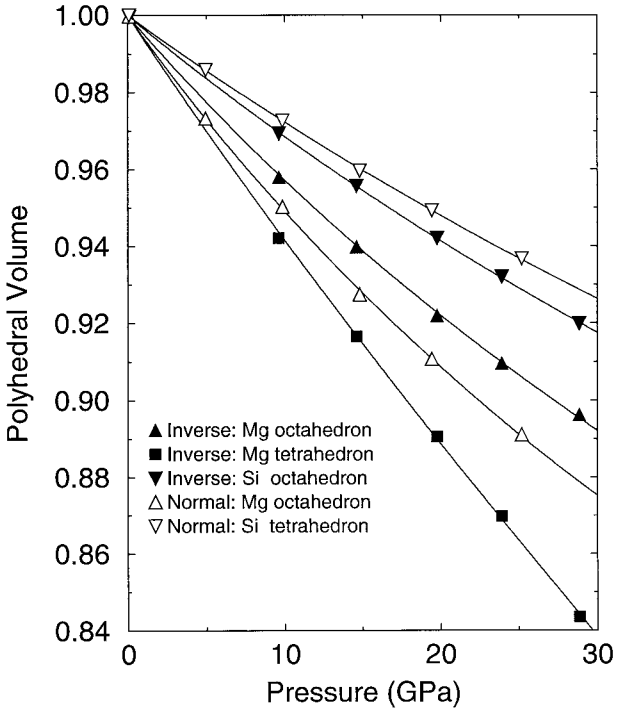

FIGURE 3. Compressibility of the individual coordination polyhedra calculated at 0 K in ringwoodite and inverse ringwoodite. The graph for tetrahedral Mg has been drawn using the parameters given in the footnote to Table 3.

To address the compression mechanism in normal and inverse ringwoodite, we determined the volume and the geometry of the individual coordination polyhedra (Fig. 3, Table 2 and Table 3). In normal ringwoodite, the compression is mainly taken up by the Mg-octahedra, which have a much lower bulk modulus than the Si-tetrahedra. The Si-tetrahedra remain ideal over the whole pressure range, while the Mg-octahedra become more ideal with increasing pressure (Figs. 4a and 5a). The compressional behavior of inverse ringwoodite is very different; here the Mg-tetrahedra are most compressible (Fig. 3, Table 3). The Mg-tetrahedra have the lowest bulk modulus, approximately 45% lower than the Mg-octahedra and a fac-

TABLE 3. Polyhedral bulk moduli of Mg_2SiO_4 in units of GPa

Coordination	Theory, ringwoodite at 0 K* Normal	Theory, ringwoodite at 0 K* Inverse	Experiment†
Mg-octahedra	173	209	150
Si-octahedra	–	294	320
Mg-tetrahedra‡	–	116	120§
Si-tetrahedra	337	–	>250

* Determined at 0 K and assuming $K_0' = 4$.
† Hazen et al. (1979) and references therein for various structures at ambient conditions.
‡ Best fit was obtained for $V_0 = 3.673$ Å^3, $K_0 = 161$ GPa, $K_0' = 1.25$.
§ For $MgAl_2O_4$ spinel: Finger et al. (1986).

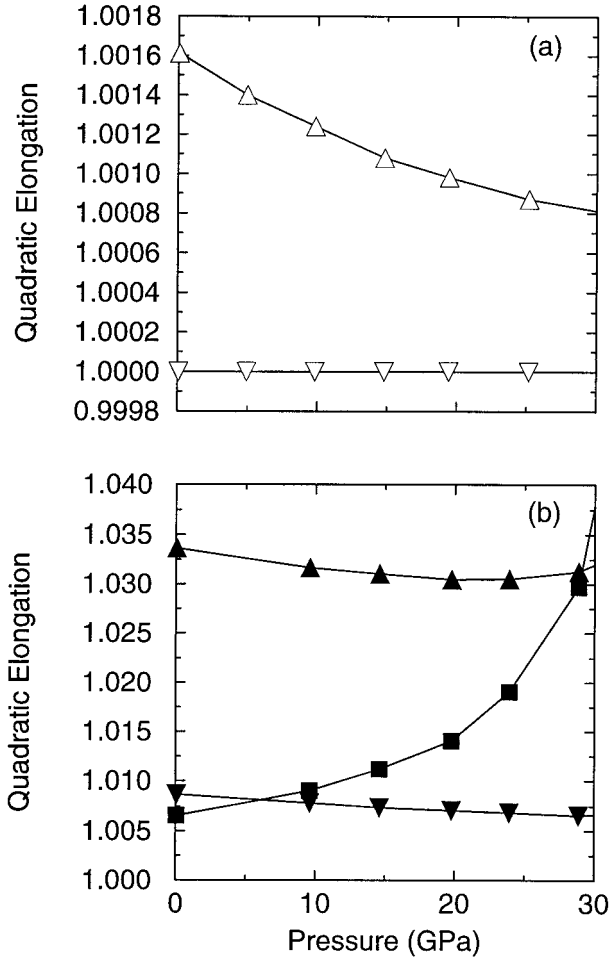

FIGURE 4. Quadratic elongation of the coordination polyhedra calculated at 0 K. (**a**) ringwoodite, (**b**) inverse ringwoodite. Symbols given in Figure 3.

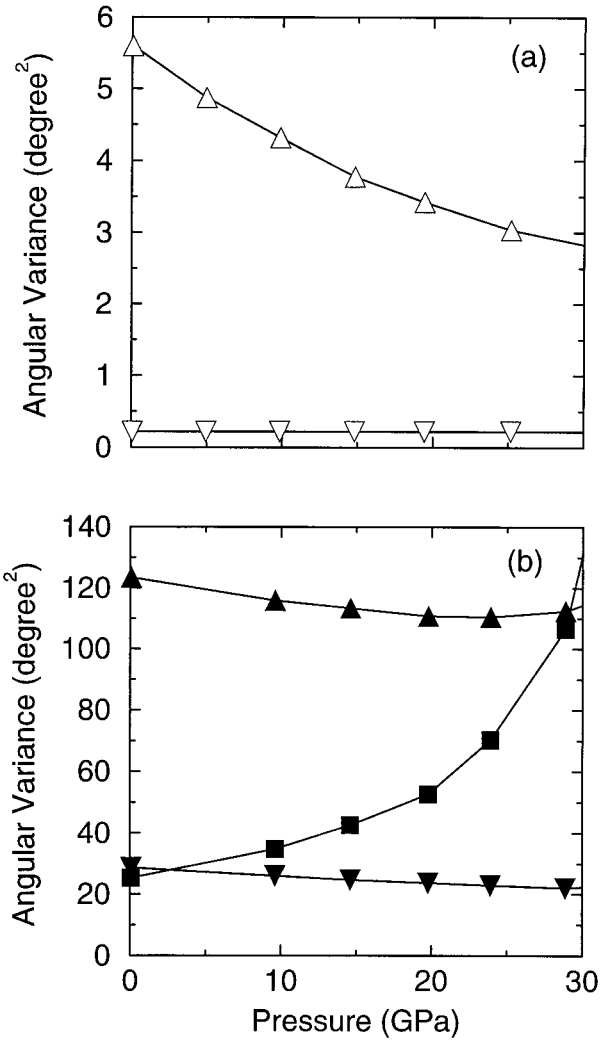

FIGURE 5. Angular variance of the polyhedral environments calculated at 0 K. (**a**) ringwoodite, (**b**) inverse ringwoodite. Symbols given in Figure 3.

tor 2.5 lower than the Si-octahedra. The distortion of the Mg and Si octahedra depends only weakly on pressure, while the Mg-tetrahedra become more distorted with increasing pressure (Fig. 4b, Fig. 5b).

Energetics of normal and inverse ringwoodite

We calculated the enthalpy difference between normal and inverse ringwoodite as a function of pressure to evaluate the effect of cation exchange on the energetics in ringwoodite. We found that the enthalpy difference between normal and inverse ringwoodite only depends weakly on pressure (Fig. 6) and is a factor of 80 smaller than the prediction by O'Neill and Navrotsky (1983). This discrepancy is discussed below. To illuminate the source of this discrepancy, we consider the effect of cation exchange alone without the structural relaxation (Fig. 7). The resulting enthalpy difference is a factor of 2.5 lower than the prediction by O'Neill and Navrotsky (1983). Comparing the unrelaxed and relaxed enthalpy differences as derived from our first-principle calculations show that the relaxed enthalpy difference is a factor of 30 smaller than the unrelaxed enthalpy difference.

DISCUSSION

Our results show that, at low temperature, normal ringwoodite is more stable than inverse ringwoodite over the whole pressure range up to 25 GPa, although inverse ringwoodite is more compressible than ringwoodite (Table 1, Fig. 1). The equation of state as derived from theory and low temperature experiments (Meng et al. 1994) are in good agreement (Fig. 1, Table 1). The zero pressure volume and bulk modulus for ringwoodite and inverse ringwoodite differ by 2.4 and 11%, respectively. A comparison to volume-bulk modulus systematics (Hazen and Finger 1979) indicate that for isostructural compounds the relative change in bulk modulus should be three to four times larger than the relative change in zero pressure vol-

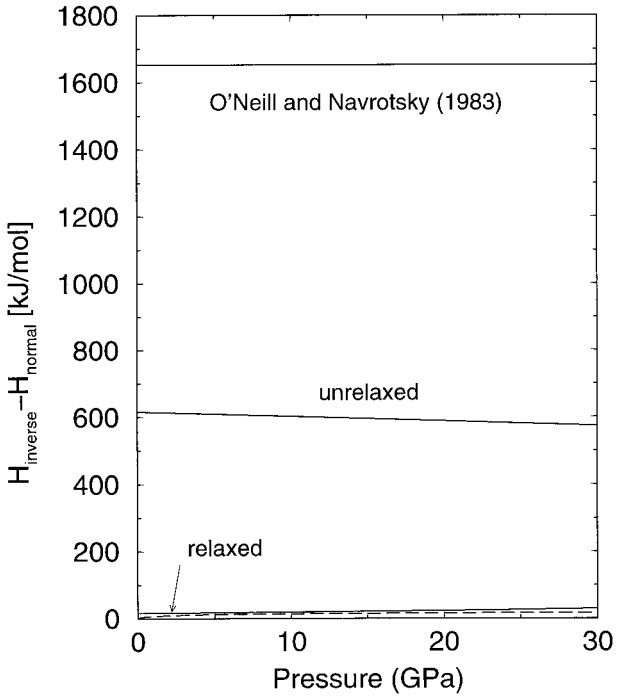

FIGURE 6. Predicted (O'Neill and Navrotsky 1983) and calculated enthalpy difference for ringwoodite and inverse ringwoodite. The geotherm (dashed line) has been taken from Stacey (1992).

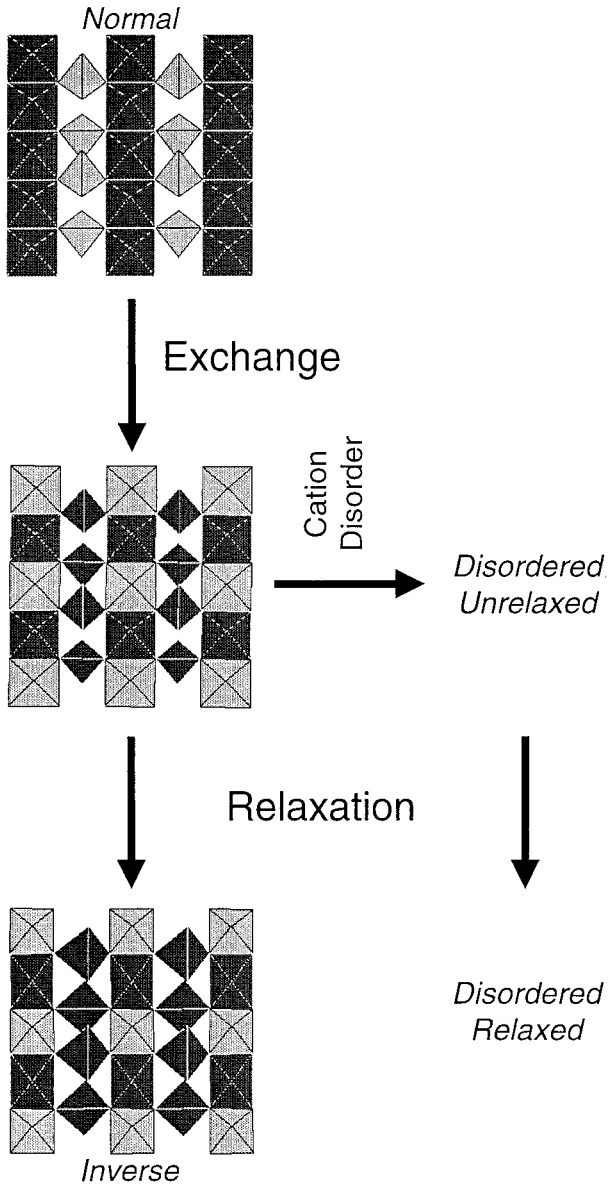

FIGURE 7. Schematic representation of the different effects that were considered to evaluate the unrelaxed and relaxed enthalpy differences between ringwoodite and inverse ringwoodite.

ume, in marginal agreement with our result. Systematics and our results contrast to experiments on pseudobrookite-type $MgTi_2O_5$, where the volume change of 0.6% upon disordering induced a change in bulk modulus of 5% (Hazen and Yang 1997).

The compression mechanisms for normal ringwoodite and inverse ringwoodite are very different. In ringwoodite, the Mg octahedra are much softer than the Si tetrahedra, whereas in inverse ringwoodite the Mg tetrahedra are softest, much softer than the Mg and Si octahedral sites (Fig. 3 and Table 3). The reason for this behavior in inverse ringwoodite can be found in the connectivity of the different polyhedra. The octahedra form a continuous edge-sharing network whereas the Mg tetrahedra share only corners with the surrounding polyhedra. Therefore it is much easier to deform the Mg tetrahedra; whose compressibility can also be seen in the quadratic elongation and the angular variance. Because the compression of the continuous network of octahedra must be accomplished against the combined bond strength of Si and Mg, it is much easier to deform the Mg tetrahedra, which is determined by the Mg bond strength alone.

Our calculated enthalpy difference between normal and inverse ringwoodite allows us to draw conclusions about the thermodynamics of ringwoodite at transition zone conditions. The enthalpy difference between normal ringwoodite and inverse ringwoodite increases with pressure (Fig. 6) by 0.73 kJ/(mol·GPa). First, we describe cation exchange in ringwoodite by referring to the formula of the intermediate, $Mg^{VI}_{2-x}Mg^{IV}_{x}Si^{VI}_{x}Si^{IV}_{1-x}O_4$, where x ranges from 0 for normal ringwoodite to 1 for inverse ringwoodite. The free energy of ringwoodite can be written in terms of x:

$$G(x, P, T) = (1 - x)G_{\text{normal}} + xG_{\text{ordered,inverse}} - TS^{IV}_{\text{conf}}(x) - TS^{VI}_{\text{conf}}(x) + H_{xs}(x, P, T) \quad (1)$$

with

$$S^{IV}_{\text{conf}}(x) = -R[x \ln x + (1 - x) \ln(1 - x)] \quad (2)$$

and

$$S^{VI}_{conf}(x) = -2R[x/2 \ln(x/2) + (2 - x)/2 \ln((2 - x)/2)] \quad (3)$$

where $H_{XS}(x, P, T)$ describes the enthalpy change due to cation disorder. The free energy difference between normal and completely inverse ringwoodite can therefore be written as:

$$G_{inverse} - G_{normal} = G_{ordered;inverse} - G_{normal} - 2RT \ln 2 + H_{XS}(1, P, T) \quad (4)$$

Assuming that the lattice contribution to the entropy does not depend strongly on the degree of inversion (O'Neill and Navrotsky 1983), we can calculate the temperature at which inverse ringwoodite becomes more stable than normal ringwoodite

$$T = \frac{\Delta H + H_{XS}}{2R \ln 2} \quad (5)$$

We have calculated $\Delta H = H_{ordered - inverse} - H_{normal}$ (Fig. 6), but cannot constrain H_{XS} directly. Assuming $H_{XS} \ll \Delta H$ we can calculate the temperature at which inverse ringwoodite becomes more stable than normal ringwoodite. At zero pressure and 20 GPa, we find $T = 1400$ K and $T = 2600$ K, respectively. This temperature is greater than expected temperatures in the transition zone. It is therefore unlikely that pure inverse ringwoodite is stable under transition zone conditions. However, there might be a considerable amount of inverse content present ($x > 0$). The inverse content depends on H_{XS} and although the value of H_{XS} is uncertain, it appears from the thermochemistry of other spinels (O'Neill and Navrotsky 1983) that H_{XS} is positive. This indicates that $T = 2600$ K is a lower limit for the temperature at which inverse ringwoodite becomes more stable than normal ringwoodite.

The enthalpy difference for normal and inverse ringwoodite as derived from our first principle calculations (Fig. 6) is smaller by a factor 80 than predicted by O'Neill and Navrotsky (1983). This discrepancy can be attributed to two factors in their work: First, structural relaxation was not considered and second, the use of a fully ionic model in the nearest neighbor approximation was used, which results in unrealistic estimates of enthalpy differences. To address the importance of these two factors, we evaluated the enthalpy difference due to cation exchange alone (Fig. 7). The resulting enthalpy difference is a factor 2.5 lower as compared to the value predicted by O'Neill and Navrotsky (1983) (Fig. 6). The remaining difference is attributed to their neglect of relaxation.

Comparing the relaxed and the unrelaxed enthalpy difference, as derived from our model, shows that the latter is larger than the former by a factor 30. It is therefore essential to include structural relaxation in models that address the energetics of cation exchange, at least in the case of ringwoodite.

Acknowledgments

This work was supported by the National Science Foundation under grants EAR-9628199 (L.P.S.) and EAR-9628042 (R.M.W.), and by the Minnesota Supercomputer Institute.

References cited

Anderson, D.L., and Anderson, O.L. (1970) The bulk modulus-volume relationship for oxides. Journal of Geophysical Research, 75, 3494–3500.

Ceperley, D.M. and Alder, B.J. (1980) Ground state of the electron gas by a stochastic method. Physical Review Letters, 45, 566–569.

Cohen, M.L. (1982) Pseudopotentials and total energy calculations. Physical Scripta. T1, 5–7.

Finger, L.W., Hazen, R.M., and Hofmeister, A.M. (1986) High pressure crystal chemistry of spinel ($MgAl_2O_4$) and magnetite (Fe_3O_4): comparisons with silicate spinels. Physics and Chemistry of Minerals, 13, 215–230.

Hazen, R.M. and Finger, L.W. (1979) Bulk modulus-volume relationship for cation-anion polyhedra. Journal of Geophysical Research, 84, 6723–6728.

——— and ———. (1979) Bulk modulus-volume relationship for cation-anion polyhedra. Journal of Geophysical Research, 84, 6273–6278.

Hazen, R.M. and Navrotsky, A. (1996) Effects on pressure on order-disorder reactions. American Mineralogist, 81, 1021–1035.

Hazen, R.M. and Yang, H. (1997) Increased compressibility of pseudobrookite-type $MgTi_2O_5$ caused by cation disorder. Science, 277, 1965–1967.

Hazen, R.M., Downs, R.T., Finger, L.W., and Ko, J. (1993) Crystal chemistry of ferromagnesian silicate spinels: Evidence for Mg-Si disorder. American Mineralogist, 78, 1320–1323.

Ita, J. and Stixrude, L. (1992) Petrology, elasticity and composition of the mantle transition zone. Journal of Geophysical research, 97, 6849–6866.

Karato, S. (1997) Seismic anisotropy in the deep mantle, boundary layers and the geometry of mantle convection. In Plomerova J., Babuska, V. N., and Libermann, R.C., Eds., Geodynamics of the Lithosphere and the Earth's Mantle.

Kiefer, B., Stixrude, L., and Wentzcovitch, R.M. (1997) Calculated elastic constants and anisotropy of Mg_2SiO_4 spinel at high pressure. Geophysical Research Letters, 24 (22), 2841–2844.

Kohn, W. and Sham, L.J. (1965) Self-consistent equations including exchange and correlation effects. Physical Review, 140, A1133–A1138.

Meng, Y., Fei, Y., Weidner, D., Gwanmesia, G.D., and Hu, J. (1994) Hydrostatic compression of γ-Mg_2SiO_4 to mantle pressures and 700 K: thermal equation of state and related thermodynamic properties. Physics and Chemistry of Minerals, 21, 407–412.

Monkhorst, H.J. and Pack, J.D. (1976) Special points for Brillouin-zone integrations. Physical Review B (13), 5188–5192.

O'Neill, H.St.C. and Navrotsky, A. (1983) Simple spinels: crystallographic parameters, cation radii, lattice energies and cation distribution. American Mineralogist, 89, 181–194.

Pickett, W.E. (1989) Pseudopotentials in condensed matter systems. Computational Physics Reports, 9, 115–197.

Sasaki, S., Prewitt, C.T., Sato, Y., and Ito, E. (1982) Single crystal x-ray study of γ-Mg_2SiO_4. Journal of Geophysical Research, 87, 7829–7832.

Stacey, F.D. (1992) Physics of the earth (2nd edition), p. 1–513, Brookfield Press.

Troullier, N. and Martins, J.L. (1991) Efficient pseudopotentials for plane-wave calculations. Physical Review B, 43, 1993–2003.

Wechsler, B.A. and Von Dreele, R.B. (1989) Structure refinements of Mg_2TiO_4, $MgTiO_3$ and $MgTi_2O_5$ by time-of flight neutron powder diffraction. Acta-Crystallographica B, 45, 542–549.

Wentzcovitch, R.M. (1991) Invariant molecular dynamics approach to structural phase transitions. Physical Review B, 44, 2358–2361.

Wentzcovitch, R.M. and Price, G.D. (1996) High pressure studies of mantle minerals by *ab initio* variable cell shape molecular dynamics. In B. Silvi and P. Darco, Eds., Molecular Engineering, p. 39–61. Kluwer, Dordrecht.

Wentzcovitch R.M. and Stixrude, L. (1997) Crystal chemistry of forsterite: a first principle study. American Mineralogist, 82, 663–671.

Wentzcovitch, R.M., Martins, J.L., and Price, G.D. (1993) Ab initio molecular dynamics with variable cell shape: application to $MgSiO_3$-perovskite. Physical Review Letters, 70, 3947–3950.

Wentzcovitch, R.M., da Silva, C.R.S., Chelikowsky, J.R., and Binggeli, N. (1998) Phase transition in quartz near the amorphization transformation. Physical Review Letters, 80, 2149–2152.

Manuscript received June 10, 1998
Manuscript accepted September 22, 1998
Paper handled by Robert M. Hazen